⌘ *Author's Choice*

THE JOURNAL OF BIOLOGICAL CHEMISTRY VOL. 285, NO. 43, pp. 32897–32905, October 22, 2010

The Viral Oncoprotein Tax Sequesters DNA Damage Response Factors by Tethering MDC1 to Chromatin*

Received for publication, May 19, 2010, and in revised form, August 19, 2010 Published, JBC Papers in Press, August 20, 2010, DOI 10.1074/jbc.M110.146373

S. Mehdi Belgnaoui, Kimberly A. Fryrear, Julius O. Nyalwidhe, Xin Guo, and O. John Semmes[1]

From the Department of Microbiology and Molecular Cell Biology, Cancer Biology and Infectious Disease Research Center, Eastern Virginia Medical School, Norfolk, Virgina 23508

Infection with human T-cell leukemia virus induces cellular genomic instability mediated through the viral oncoprotein Tax. Here we present evidence that Tax undermines the cellular DNA damage response by sequestration of damage response factors. We show by confocal microscopy that Tax forms damage-independent nuclear foci that contain DNA-PK, BRCA1, and MDC1. Tax sequesters MDC1 to chromatin sites distinct from classic ionizing radiation-induced foci. The recruitment of MDC1 is competitive between the two foci. The N-terminal region of Tax is sufficient for foci localization, and the C-terminal half is critical for binding to MDC1 and recruitment of additional response factors. Tax expression and DNA damage response factor recruitment repressed the formation of ionizing radiation-induced Nbs1-containing foci. The Tax-induced "pseudo" DNA damage response results in phosphorylation and monoubiquitylation of H2AX, which is ablated by siRNA suppression of MDC1. These data support a model for virus-induced genomic instability in which viral oncogene-induced damage-independent foci compete with normal cellular DNA damage response.

Viruses have developed many host interaction strategies to acquire control of their environment. Some virus-host relationships progress through oncogenesis and result in cellular transformation. Among the so-called "transforming retroviruses," the human T-cell leukemia virus, type I (HTLV-1)[2] displays a unique path through oncogenesis. HTLV-1 is the causative agent for adult T-cell leukemia, an aggressive leukemia/lymphoma. Infection by HTLV-1 is characterized by a long asymptomatic period of on average ~30 years (1). Over this period of time ~3% will develop adult T-cell leukemia (2). The viral transactivator protein Tax has been shown to transform fibroblasts (3, 4) and T-cell isolates (5) and to spontaneously immortalize primary T-cells (6). The molecular details of the transformation process are not completely understood, but mounting evidence supports the hypothesis that Tax induces genomic instability in the host, a condition that accelerates accumulation of mutations that support cellular transformation (7, 8). In fact, Tax expression directly correlates with the presence of genomic instability in pretransformed infected T-cells examined *ex vivo* (9).

We and others have proposed that Tax disrupts genomic integrity by repressing aspects of the cellular DNA damage response (DDR). Support for this hypothesis derives primarily from studies demonstrating that Tax expression results in increased cellular mutational frequency (10, 11), inhibition of DNA repair (12–14), and uncoupling of checkpoint control (15–18). Sustained deficiencies of this sort are expected to result in genomic instability, and this hypothesis is consistent with the observation that genomic instability characterizes pretransformed HTLV-infected cells and the long asymptomatic period prior to transformation.

An important cellular strategy for coordination of an efficient DDR is through the sequential recruitment of repair-response factors to the sites of DNA damage. The formation of these damage foci result from cellular efforts to consolidate repair activity and as such the formation, enumeration/size, and persistence of the foci reflect regulation of DDR (19–21). The best studied of these nuclear structures is ionizing radiation-induced foci (IRIF). Immediately following insult by ionizing radiation, damaged DNA ends are recognized by the Mre11-Rad50-Nbs1 (MRN) complex. This recognition step is critical to the initial activation of DNA-PK/ATM, which sets in motion the activation of a number of downstream signal mediators such as Chk2, BRCA1, and 53BP1. The signaling coincides with recruitment of factors to the sites of damage, a process that is iterative and tied to the extent of damage. Recently, the recruitment of MDC1 (mediator of DNA damage checkpoint protein 1) to IRIF has been revealed as a critical event for initiation, amplification, and stabilization of the foci at sites of damage (22–28). The mobilization and coordination of IRIF formation is achieved in large part by ubiquitin-mediated events following the recruitment of the E3 ligase RNF8 (ring finger protein 8) by MDC1 to the foci (29–32).

In the present study we demonstrate that Tax tethers MDC1 to chromatin overlapping with nuclear foci called Tax speckled structures (TSS). The TSS foci and IRIF do not colocalize, and recruitment of MDC1 is competitive between the two sites. We show that TSS contain the DDR proteins DNA-PK, BRCA1, and MDC1 and that Tax expression alone generates a DDR signal that is dependent upon the sequestration of MDC1. Tax expression and formation of TSS foci impaired the normal DDR

* This work was supported by Public Health Service Grant CA76959 (to O. J. S.) from the National Cancer Institute.

⌘ *Author's Choice*—Final version full access.

[1] To whom correspondence should be addressed: Cancer Biology and Infectious Disease Research Center, Dept. of Microbiology and Molecular Cell Biology, Eastern Virginia Medical School, 700 West Olney Rd., Norfolk, VA 23508. Tel.: 757-446-5904; Fax: 757-446-5766; E-mail: Semmesoj@evms.edu.

[2] The abbreviations used are: HTLV-1, human T-cell leukemia virus, type I; DDR, DNA damage response; IR, ionizing radiation; IRIF, IR-induced foci; MRN, Mre11-Rad50-Nbs1; TSS, Tax speckled structure(s); Gy, gray; mono-ub-γ-H2AX, monoubiquitylation of γ-H2AX.

as demonstrated through a quantitative reduction in damage-induced Nbs1-containing foci. These results support a novel competition model for Tax-induced genomic instability.

EXPERIMENTAL PROCEDURES

Cell Culture and Transient Transfection—293T cells were maintained at 37 °C in a humidified atmosphere of 5% CO_2 in Iscove's modified Dulbecco's medium supplemented with 10% fetal bovine serum (Cambrex, East Rutherford, NJ) and 1% penicillin-streptomycin (Invitrogen). Transfections of 293T cells were performed by standard calcium phosphate precipitation.

Plasmids and Antibodies—Generation of the *STaxGFP*, *STax*, and *SGFP* plasmids has been described (33). *HA*-tagged human *MDC1* (pcDNA3-neo) was a gift from D. Lukas (Danish Cancer Society, Copenhagen, Denmark).

For immunofluorescence analysis we used the following antibodies: anti-MDC1 goat polyclonal (1/100; Santa Cruz Biotechnology, Santa Cruz, CA), anti-BrdU mouse monoclonal (1/50; BD Biosciences, San Jose, CA), anti-BRCA1 mouse monoclonal (1/100; Santa Cruz Biotechnology), anti-Nbs1 rabbit polyclonal (1/400; Novus Biologicals, Littleton, CO), and anti-DNA-PK Thr(P)^{2609} mouse monoclonal (1/400; Abcam, Cambridge, MA). For Western analysis, the following antibodies were used: anti-MDC1 goat polyclonal (1/200; Santa Cruz Biotechnology), anti-GFP mouse monoclonal (1/500; Santa Cruz Biotechnology), anti-HA rabbit polyclonal (1/1500, Zymed Laboratories Inc., San Francisco, CA), anti-tubulin mouse monoclonal (1/2000; Sigma), anti-Tax-pep3 rabbit polyclonal (1/2000), anti-ORC2 rabbit polyclonal (1/400; Santa Cruz Biotechnology), and anti-γ-H2AX (1/2000; R & D Systems, Minneapolis, MN).

siRNA Transfection—The cells were plated at 2×10^5 cells/ml in 60-mm plates. The following day the medium was replaced with serum-free and antibiotic-free medium 1 h prior to transfection. A total of 100 pmol of siRNA MDC1 (Santa Cruz Biotechnology) or siRNA control were diluted in 500 μl of Opti-MEM® I medium without serum. Lipofectamin™ 2000 was gently mixed, and 5 μl was diluted in 500 μl of Opti-MEM® I medium without serum. The mixture was mixed and incubated for 5 min at room temperature. The selected DNA and/or siRNA were mixed with the diluted Lipofectamin™ 2000 and incubated for 20 min at room temperature. The DNA-siRNA-Lipofectamin™ 2000 complexes were then added to the plate. The plates were then incubated at 37 °C for 6 h, washed, and plated with complete medium. The cells were harvested after an additional 48 h.

Immunofluorescence Confocal Microscopy—The cells were transfected directly upon coverslips. The medium was removed, and the coverslips were washed twice with ice-cold PBS. The cells were fixed with 4% paraformaldehyde for 12 min at room temperature. The fixed cells were then washed three times with PBS and incubated with ice-cold methanol for 2 min. The coverslips were then washed four times with PBS and incubated with primary antibody diluted in 3% BSA in PBS. Excess primary antibody was removed with two washes each of PBS, 1% Tween 20 and PBS. The coverslips were then incubated with species-specific Alexa Fluor 594-conjugated secondary antibody (Invitrogen) diluted at 1/1000 in 3% BSA in PBS. The nuclei were counterstained with To-Pro-3 iodide (Invitrogen) diluted 1/1,000 in the same secondary antibody solution. Excess secondary antibody was removed with two washes each of 3% BSA in PBS and PBS. One drop of Vectashield mounting medium with DAPI (Vector Laboratories Inc., Burlingame, CA) was placed onto a slide, and the coverslip was inverted onto the slide and left to air dry for 1 h at room temperature in the dark. Confocal fluorescent images were acquired using a Zeiss LSM 510 confocal microscope at 63× magnification with a 2× zoom using argon (488 nm), HeNe1 (543 nm), and HeNe2 (633 nm) lasers and imaged with LSM Image Browser software (Carl Zeiss, Jena, Germany).

Immunoblot Analysis—Proteins separated by SDS-PAGE were transferred to Immobilon-P membranes (Millipore, Billerica, MA) using the semi-dry transfer method with 20 V applied for 1 h. The membranes were then blocked for 1 h at room temperature in 1× Odyssey blocking buffer (Li-Cor Biosciences, Lincoln, NE). Primary antibodies diluted in 1× Odyssey blocking buffer were applied to the membranes and incubated at 4 °C overnight with shaking. The membranes were washed four times for 5 min with PBS, 1% Tween 20. Li-Cor Odyssey secondary antibodies were diluted to a concentration of 1/20,000 in 1× Odyssey blocking buffer containing 0.5% SDS and 0.5% Tween and then incubated for 1 h at room temperature protected from light. The membranes were washed four times for 5 min with PBS, 1% Tween 20 and then stored in PBS until ready to be analyzed. The blots were scanned and analyzed with a Li-Cor Odyssey scanner and software.

Isolation of Cellular Chromatin Fraction—Approximately 5×10^6 cells were rinsed twice with ice-cold PBS and harvested with a cell scraper into 1 ml of ice-cold PBS. The cells were centrifuged at 1500 rpm for 2 min, the supernatant was discarded, and the cell pellet was resuspended in ice-cold PBS. The cells were again centrifuged, and the pellet was resuspended in 200 μl of buffer A (100 mM HEPES, pH 7.9, 10 mM KCl, 1.5 mM $MgCl_2$, 0.34 M sucrose, 10% glycerol, 10 mM NaF, 1 mM Na_2VO_3, 1 mM DTT, and protease inhibitor mixture) with a blunt 1000-μl micropipette tip. Triton X-100 was added to a final concentration of 0.1%, and the solution was incubated on ice for 5 min. The solution was then centrifuged at 1,300 × *g* (4000 rpm) at 4 °C for 5 min in a 1.5-ml centrifuge tube. The supernatant (fraction S1) was separated from the pellet (fraction P1), which contains the nuclei. Fraction S1 was clarified by high speed centrifugation at 20,000 × *g* (14,000 rpm) at 4 °C for 5 min. The supernatant (fraction S2), which represents the cytosolic fraction, was collected, and the pellet was discarded. Fraction S2 was stored at −80 °C until ready to use. Pellet fraction P1 was washed once with buffer A (0.6 ml/tube) by centrifugation again at 4000 rpm at 4 °C for 5 min. Washed fraction P1 was resuspended in 100 μl of buffer B (3 mM EDTA, 0.2 mM EGTA, 1 mM DTT, protease inhibitor mixture) with a blunt 1000-μl micropipette tip and lysed for 30 min on ice. The P1 sample was then centrifuged at 1,700 × *g* (5000 rpm) at 4 °C for 5 min. The resulting supernatant (fraction S3), which contains the soluble nuclear proteins, was separated from the pellet (fraction P2) that contains the chromatin. Fraction S3 was stored at −80 °C until ready to use. Fraction P2 was washed once with Buffer B (0.6 ml/tube) by centrifugation at 10,000 × *g*

(11,000 rpm) at 4 °C for 1 min. Fraction P2 was then resuspended in M-PER (Thermo-Fisher Scientific, Rockford, IL) protein extraction buffer (180 μl/sample), briefly sonicated, and clarified by high speed centrifugation at 20,000 × *g* (14,000 rpm) at 4 °C for 5 min. The final supernatant (fraction P3), which contains the chromatin-bound proteins, was collected and kept at −80 °C until ready to use.

Labeling Damage Foci by Incorporation of BrdU—Mock and *STaxGFP* transfected cells were incubated with 10 μg/ml of BrdU (Sigma) for 30 h under normal cell culture conditions and then exposed to 15 Gy of x-ray irradiation or left untreated. After ionizing radiation, the cells were grown for 16 h, washed with PBS, fixed with methanol for 5 min at −20 °C, and blocked with 3% BSA for 30 min. The cells were immunostained with mouse anti-BrdU followed by anti-mouse Alexa Fluor 594-conjugated secondary antibody (Invitrogen). The nuclei were counterstained with To-Pro-3 iodide (Invitrogen) diluted at 1/1,000.

RESULTS

Tax Colocalizes with DDR Proteins—We previously described the subcellular localization of Tax to prominent nuclear speckles we termed TSS (34) and have subsequently demonstrated the recruitment of Chk2 and DNA-PK to TSS by Tax (15, 35, 36). These observations and the knowledge that Tax expression results in genomic instability led us to speculate that Tax induces genomic instability via functional sequestration of proteins of the cellular DDR. To advance this hypothesis, we examined additional DDR proteins for colocalization to TSS. Tax-GFP fusion protein was transiently expressed, and endogenous DDR proteins were analyzed for colocalization using indirect immunofluorescence confocal microscopy. In Fig. 1, we show a typical expression pattern of Tax localized to nuclear TSS. The phosphatidylinositol 3-kinase damage response activator DNA-PK, activated via phosphorylation at Thr^{2609}, colocalizes with TSS as we have previously demonstrated (33). In addition, we now show that the DDR mediator proteins BRCA1 and MDC1 also localize to TSS. Greater than 80% of all nuclei counted showed colocalization between TSS and the indicated protein. Foci for BRCA1, DNA-PK, and MDC1 were observed in the absence of Tax expression in less than 5% of cells. The localization of nucleolin to a nuclear domain distinct from TSS is included as a control. The recruitment of MDC1 to TSS is especially interesting given the critical role this protein plays in the initiation and amplification of DDR, and IRIF formation and maintenance. These findings establish that Tax-induced TSS foci are enriched for DDR proteins.

TSS and IRIF Are Separate Nuclear Structures—To gain insight into the formation of TSS, it was critical to determine whether the TSS were independent/separable from classic DDR structures such as IRIF. Because TSS share many of the protein markers of IRIF, we utilized a modified BrdU staining technique that detects DNA breaks to visualize damage foci (37). Tax-expressing cells were pulsed with BrdU for 30 h before ionizing radiation treatment to completely label the DNA. No denaturation step was used before anti-BrdU staining; therefore only the accessible BrdU epitopes that occur at

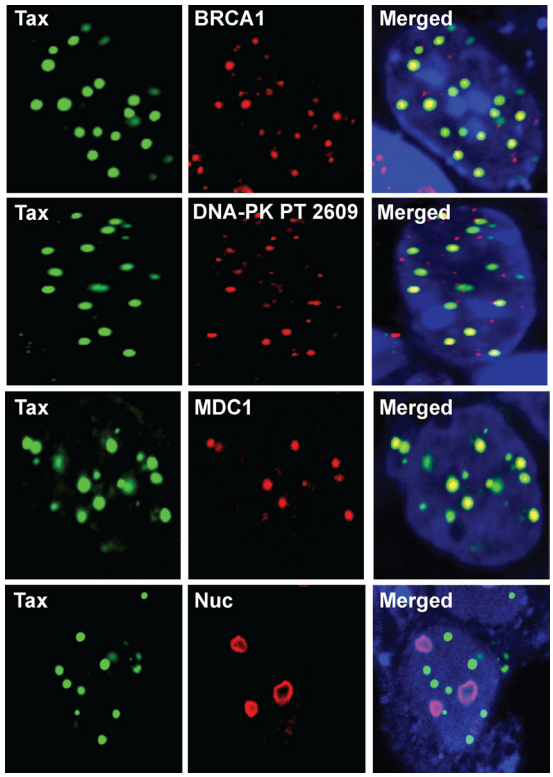

FIGURE 1. **Tax colocalizes with DDR proteins.** The cells were transiently transfected to express Tax-GFP, fixed, and subsequently subjected to indirect immunofluorescence confocal microscopy for the coexpression of BRCA1 (*top row*), DNA-PK $Thr(P)^{2609}$ (*PT 2609*, *second row*), MDC1 (*third row*), and nucleolin (*bottom row*). Shown for each condition is a representative of 25 nuclei containing TSS. Each row consists of the same field of view using the *green* (Tax), *red* (indicated protein), and merged channels. The cells were also counterstained with TO-PRO displayed in the *blue* channel and included in the merged image.

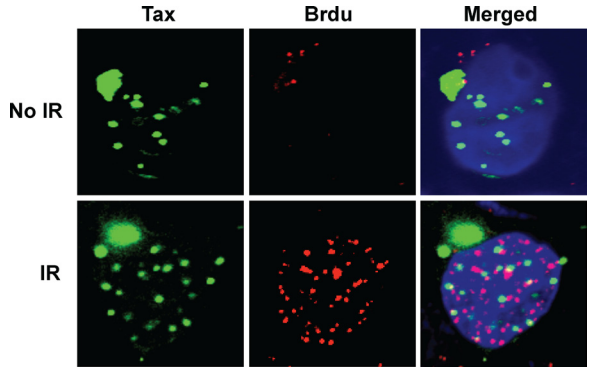

FIGURE 2. **TSS and IRIF are separable nuclear structures.** The cells were transiently transfected to express Tax-GFP, incubated with BrdU, and then prepared for indirect immunofluorescence confocal microscopy. Each row consists of the same field of view showing the *green* (Tax), *red* (BrdU), and merged channels. TO-PRO was used as a counterstain, collected in the *blue* channel, and included in the merged image. The cells in the *bottom row* were exposed to 5 Gy of IR as described. The images shown were selected as representative of the characterization of 25 nuclei for each experimental condition.

DNA strand breaks are visualized. If TSS are formed at sites of DNA damage, then we would expect to observe colocalization with the BrdU foci. As shown in Fig. 2, in the absence of exogenous irradiation, there were no nuclear BrdU foci and thus no evidence of TSS residing at sites of DNA damage. We next induced the formation of IRIF by exposing the cells to 5 Gy of IR

and examined the cells 16 h later. In the Tax-expressing cells exposed to IR clear BrdU damage, foci were observed. However, there was only incidental overlap between TSS and IRIF. Specifically, less than 50% of cells expressing both foci displayed overlap and in those cells that did, ~7% of TSS contained BrdU foci. These data demonstrate that although TSS and IRIF share many DDR proteins, they are in fact different structures.

Characterization of the IRIF and TSS—Having established that TSS and IRIF are independent structures, we hypothesized that TSS may compete with IRIF for limiting DDR proteins. This competition for limiting DDR proteins would provide a mechanism for repression of the repair response and Tax-mediated genomic instability. One approach toward identification of limiting factors is to induce both TSS and IRIF and observe the distribution of known DDR proteins. In these studies, we expressed Tax-GFP and examined the colocalization of endogenous proteins by indirect immunofluorescence confocal microscopy. We established IRIF by exposure to 5 Gy of IR to ensure maximum recruitment to IRIF. In Fig. 3 we show that MDC1, DNA-PK, and BRCA1 are all induced to localize to TSS in the absence of IR. Greater than 80% of counted cells showed colocalization of TSS and each of these nuclear foci. When both TSS and IRIF are present, DNA-PK and BRCA1 are effectively recruited to both structures in >92% of cells. However, when presented with both IRIF and TSS, MDC1 localized almost exclusively to foci outside of TSS. This result suggests that MDC1 may be a critical factor for regulating TSS/IRIF formation. Interestingly, expression of Tax did not result in induction of Nbs1 localization to TSS in the absence of IR, although we could demonstrate efficient induction and localization to IRIF. Because Nbs1 is a critical component of the damage-sensing complex MRN, the absence of Nbs1 in TSS is consistent with a lack of associated DNA breaks.

TSS and IRIF Compete for Recruitment of MDC1—Of the tested DDR proteins, MDC1 appears to localize either to TSS in the absence of IR or to IRIF in the presence of high doses of IR. We reasoned that if the localization of MDC1 to TSS and/or IRIF was competitive, then MDC1 localization would be dictated by the relative recruitment to each site. We were unable to effectively titrate IRIF directly because IR exposures less than 1 Gy resulted in inconsistent formation of IR-induced MDC1-containing foci. Therefore, to achieve a competition balance between the amount of damage *versus* the amount of Tax, we "titrated" damaged DNA by following time points post-repair. We reasoned that as damage was resolved then the "demand" for IR foci would fall below the demand for Tax foci. A standard dose of 1 Gy was found to produce sufficient IRIF and allow for cell recovery. Because the experiments were conducted within 24 h, Tax expression was relatively constant (protein half-life, >24 h). Each experimental time point resulted from analysis of 25 nuclei from cells in which both TSS and IRIF were observed. A simple numerical average was generated for the percentage of foci that overlap. In the absence of IR the colocalization of MDC1 to TSS was >84% (Fig. 4). However, at 4 h following exposure to 1 Gy of IR, MDC1 dramatically relocalized to IRIF with <9% of foci overlap. We also observed that the relative size and shape of the TSS remain unchanged throughout the experiment. At the 24-h time point the MDC1 foci outside of TSS have both reduced in number and size as is consistent with resolved DNA damage. Under these conditions, ~47% of the TSS now displayed colocalization with MDC1. Thus, as damaged DNA is repaired and the recruitment balance shifts toward TSS foci, MDC1 relocalizes to TSS.

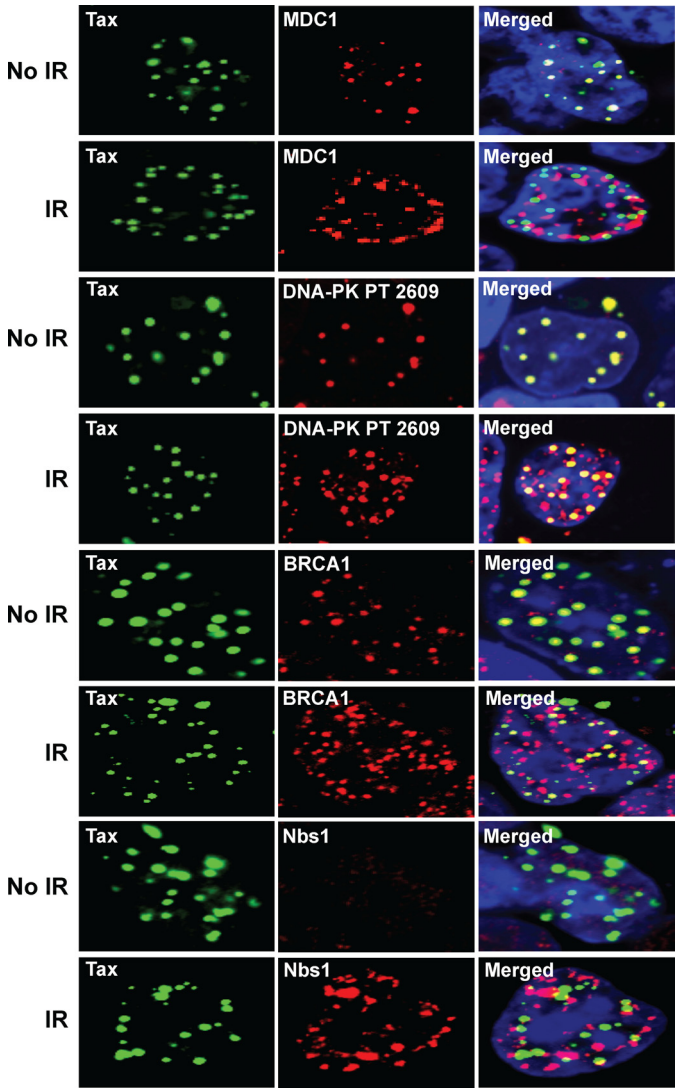

FIGURE 3. **Localization of DDR factors to TSS.** The cells were transiently transfected to express Tax-GFP, fixed, and subsequently subjected to indirect immunofluorescence confocal microscopy for the expression of MDC1, DNA-PK Thr(P)^{2609} (*PT 2609*), BRCA1, and Nbs1 (indicated). For each condition, 25 nuclei were examined in which TSS and the indicated protein were both observed. Each row consists of the same field of view using the *green* (Tax), *red* (indicated protein), and merged channels. The cells were also counterstained with TO-PRO displayed in the *blue* channel and included in the merged image. The cells were either left untreated (*No IR*) or treated with ionizing radiation (*IR*).

Tax Binds to MDC1—Damage-independent DDR foci were shown to result from tethering MDC1 to DNA (38). We thus speculated that Tax initiates a damage-independent DRR within TSS by binding to and recruiting MDC1. In this series of experiments we sought to establish whether Tax binds to MDC1.

HA-MDC1 and either *S-TaxGFP*, *S-Tax*, or *S-GFP* were cotransfected into 293T cells, and Tax complexes were subsequently isolated from whole cell lysates using S-agarose chro-

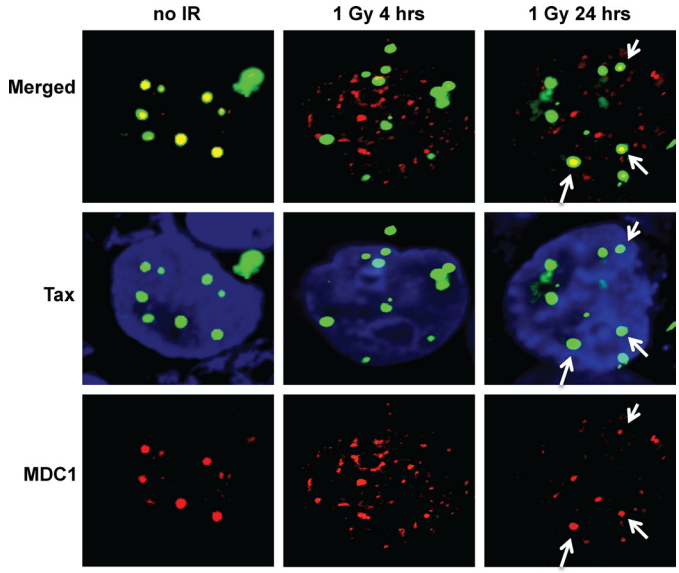

FIGURE 4. **TSS and IRIF compete for recruitment of MDC1.** The cells were transiently transfected to express Tax-GFP, fixed, and subsequently subjected to indirect immunofluorescence confocal microscopy for the expression of MDC1. Each column represents untreated cells (*no IR*) or cells treated with low dose ionizing radiation and incubated for 4 h (*1 Gy 4 h*) or 24 h (*1 Gy 24 h*). Each column contains panels from the same field of view showing *green* (Tax), *red* (MDC1), and merged images. The cells were also counterstained with TO-PRO displayed in the *blue* channel and included in the *green* channel image. The *arrows* in the last column of images are used as a reference point for colocalized foci. For each experimental point 25 nuclei displaying both TSS and MDC1 foci were counted.

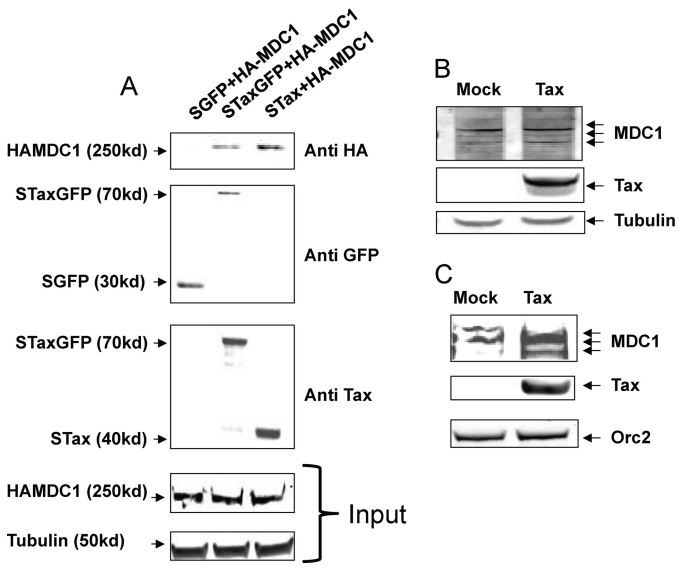

FIGURE 5. **Tax binds MDC1.** *A*, coimmunoprecipitation of Tax and MDC1. The cells were transiently transfected to express HA-MDC1 and either S-GFP, S-Tax-GFP, or S-Tax (indicated). S-tagged protein complexes were isolated and subjected to SDS-PAGE separation and Western analysis. Shown is analysis for expression of Tax and the fusion protein tags HA and GFP in the isolated complexes (indicated). Also shown is the analysis of the input prior to complex isolation for expression of HA-MDC1 and tubulin (indicated). *B*, effect of Tax on total expression of MDC1. The cells were either mock transfected or transfected to express Tax and whole cell extracts prepared and subjected to SDS-PAGE separation and analysis by Western blot. Shown is the expression of endogenous MDC1 and expressed Tax protein (indicated). Analysis for expression of tubulin was performed for normalization. *C*, Tax increases the steady-state level of MDC1 in chromatin fraction. The same cells in *B* above were subjected to chromosomal fractionation and analysis of chromatin-bound proteins. Shown is the expression of endogenous MDC1 and expressed Tax (indicated). Analysis of the chromatin protein Orc2 was performed for normalization.

matography. We directly normalized cell lysates to expression of MDC1 and adjusted expression efficiency to achieve comparable expression of Tax, Tax-GFP, or GFP. We also conducted immunoblot analysis for expression of tubulin in the extracts prior to purification of complexes for additional experimental normalization. In Fig. 5*A*, we show that both TaxGFP and Tax protein coprecipitates with MDC1 at comparable efficiency. In contrast, GFP fails to form a complex with MDC1. These results demonstrate a specific binding between Tax and MDC1.

We previously determined that TSS reside within the subnuclear architecture of interchromatin granules (34). Thus, if Tax is binding to MDC1 and recruiting this protein into TSS, then the relative amount of MDC1 within the chromatin fraction should increase in the presence of Tax. In this experiment, we isolated the cellular chromatin fraction from cells either expressing Tax or not. The isolated chromatin fractions were then separated by SDS-PAGE and immunoblotted to determine steady-state levels of endogenous MDC1. We initially determined that the total expression of MDC1 was unaffected by the expression of Tax (Fig. 5*B*). When normalized to tubulin, the total cell extracts presented with equivalent levels of MDC1. However, in the chromatin fraction the relative amount of MDC1 was dramatically increased in the Tax-expressing cells (Fig. 5*C*). As has been reported elsewhere, we see multiple forms of MDC1 with different migration rates (39). It has been speculated that these isoforms are due to differential phosphorylation (40). The chromatin extracts were normalized to expression of the chromatin-specific protein Orc2. The relative expression of tubulin and Orc2 was used to qualify the efficiency of the chromatin fractionation process. Thus, Tax-expressing cells display an increased steady-state level of endogenous MDC1 in the chromatin fraction as a result of Tax expression. This result is consistent with our model for Tax binding to MDC1 and recruiting the protein to chromatin-associated TSS.

Tax 1–75 Fails to Recruit DDR Proteins to TSS—We recently identified a TSS localization signal in Tax that is necessary and sufficient for targeting to TSS (41). Specifically, when we linked GFP to the first 75 amino acids of Tax, encompassing both the NLS (1–50) and TSS localization signal (50–75), this protein formed nuclear foci and targeted to the same subnuclear sites as wild type Tax. Having identified the minimal structure of Tax required for localization to TSS, we asked whether the TSS localization signal domain was able to recruit cellular DDR. We observed that although Tax1–75 could efficiently form TSS foci, neither MDC1 nor DNA-PK Thr(P)^{2609} was recruited to these structures (Fig. 6). We then examined the Tax 1–75 expressing cells for ability to form IRIF. The formation of IRIF and recruitment of MDC1 and DNA-PK to foci was unimpaired in these cells. In addition, the IRIF did not colocalize with the TSS. These data show that recruitment of DDR proteins to TSS requires the C-terminal half of Tax and suggests that Tax serves to bridge the formation of DDR-containing TSS.

Tax Expression and Formation of TSS Inhibit the Normal DNA Damage Response—We reasoned that if TSS and IRIF compete for MDC1 recruitment and DDR activation, then

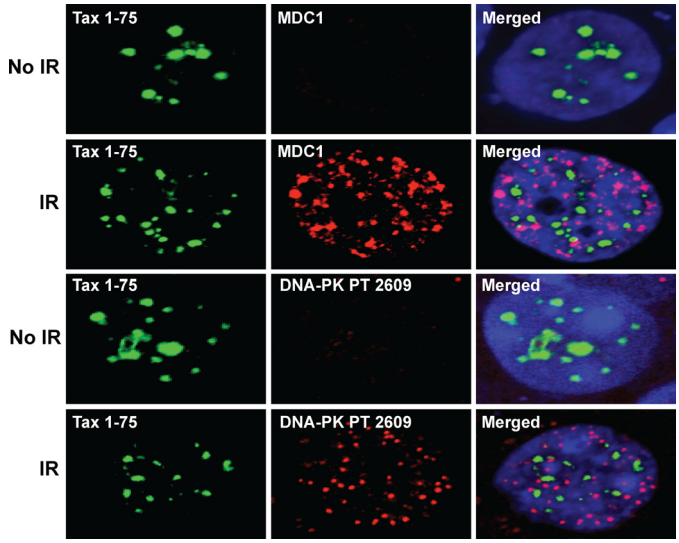

FIGURE 6. **Recruitment of DDR factors requires C-terminal half of Tax.** The cells were transiently transfected to express Tax(1–75)-GFP, fixed, and subsequently subjected to indirect immunofluorescence confocal microscopy for the expression of MDC1 and DNA-PK Thr(P)^{2609} (*PT 2609*). For each experimental condition 25 nuclei were observed. Each row consists of the same field of view using the *green* (Tax), *red* (indicated protein), and merged channels. The cells were also counterstained with TO-PRO displayed in the *blue* channel and included in the merged image. The cells were either untreated (*No IR*) or treated with ionizing radiation (*IR*).

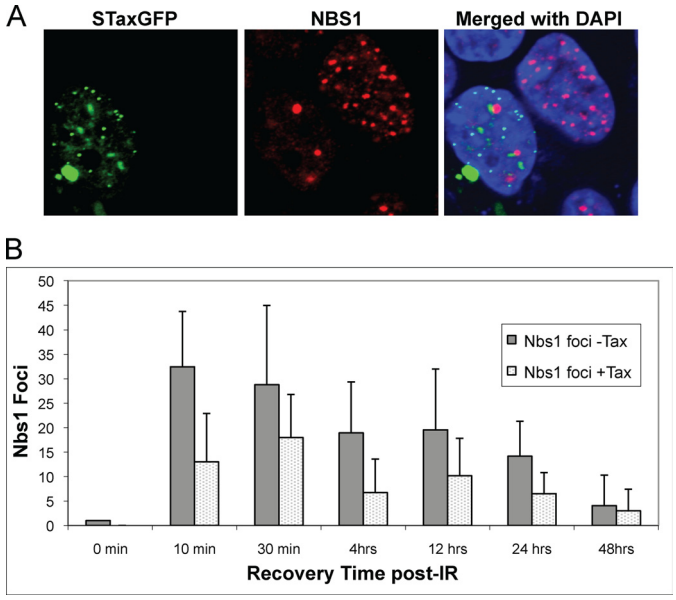

FIGURE 7. **Tax expression inhibits IRIF formation.** Transient transfection of cells was performed to achieve 25% Tax-expressing cells. *A*, a Tax-expressing cell paired with a nonexpressing cell, with well formed nuclei (*blue*) and measurable Nbs1 foci (*red*), is shown. The Tax-expressing cell (*green speckles*) is indicated. *B*, a minimum of 25 Tax-expressing cells and 25 control cells with intact nuclei were counted for each time point. The experiment was conducted in duplicate. The total number of foci/cell was determined, and an average value was plotted. This calculated foci value was recorded for each time point. The S.D. is plotted as *error bars*.

expression of Tax should impair the normal damage-induced DDR. As we noted earlier, in contrast to all other accessed DDR factors, Nbs1 was not recruited to TSS foci. Therefore, we were able to measure IRIF formation separate from TSS formation by observation of Nbs1 recruitment into IRIF. In contrast to MDC1 foci, we were able to observe a robust Nbs1-containing foci formation at lower IR doses, and so for these experiments we utilized an exposure of 0.5 Gy. Experimental observations were made by counting foci during a time course from 10 min to 48 h. In Fig. 7*A* we provide an example of the difference in the number of Nbs1 foci in Tax-expressing cells compared with control cells. In response to IR the normal cellular response is a rapid induction of Nbs1-containing foci. However, for Tax-expressing cells this number was dramatically reduced. When these observations were averaged over a sampling of the field of view, the average number of IRIF/cells was reduced in Tax-expressing cells (Fig. 7*B*). The inhibitory effect was consistent across the IRIF response spectrum with both cell types showing complete resolution at 48 h post-IR.

Activation of H2AX by Tax Is Mediated through MDC1—It has recently been shown that MDC1 is required for mono-ubiquitylation of γ-H2AX (mono-ub-γ-H2AX), a critical activation step of H2AX (42). The post-translational modification causes a change in chromatin conformation, thus "opening up" the DNA and allowing the recruitment of downstream DDR proteins. Earlier studies detected mono-ub-γ-H2AX using γ-H2AX antibodies to resolve a 25-kDa band, which is ~9 kDa (the size of one ubiquitin) larger than the 16.5-kDa γ-H2AX band (29, 43). We employed this approach to examine the effect of Tax expression on H2AX. In addition, we utilized siRNA to achieve specific suppression of MDC1 to explore the role of MDC1 in this process. In Fig. 8*A*, we show efficient suppression of MDC1 expression by siRNA. When normalized to tubulin, the steady-state levels of endogenous MDC1 were reduced when compared with treatment with control siRNA. We next expressed Tax in cells treated with either siRNA control or siRNA specific to MDC1. These cells were then harvested, and chromatin fractions were isolated. The recovery of proteins in the chromatin fraction was normalized to expression of Orc2. In Fig. 8*B*, we demonstrated that the steady-state levels of chromatin-bound endogenous MDC1 were low in the absence of Tax, and siRNA suppression modestly reduced those levels. However, we observed an increase in chromatin-bound endogenous MDC1 following Tax expression. The activity of H2AX, as determined by presence of mono-ub-γ-H2AX, was correspondingly low in the absence of Tax. In the presence of Tax, we observed an increase in γ-H2AX at 16.5 kDa and the presence of a 25-kDa band corresponding to mono-ub-γ-H2AX.

We next demonstrated that we could efficiently knock down chromatin-bound MDC1 in Tax-expressing cells. The siRNA treatment had no effect on the steady-state levels of Tax or endogenous Orc2. The specific suppression of MDC1, however, did correlate with a reduction in the levels of γ-H2AX and a dramatic decrease in the levels of mono-ub-γ-H2AX in Tax-expressing cells. When normalized to Tax expression there was a greater than 6-fold decrease in mono-ub-γ-H2AX. Thus, we clearly show that Tax alone can initiate a DDR as evidenced by activated H2AX. We also show that MDC1 is required to mediate this Tax response.

DISCUSSION

The only known human tumor retrovirus, HTLV-1, achieves cellular transformation through mechanisms that do not involve delivery or insertional activation of a cellular onco-

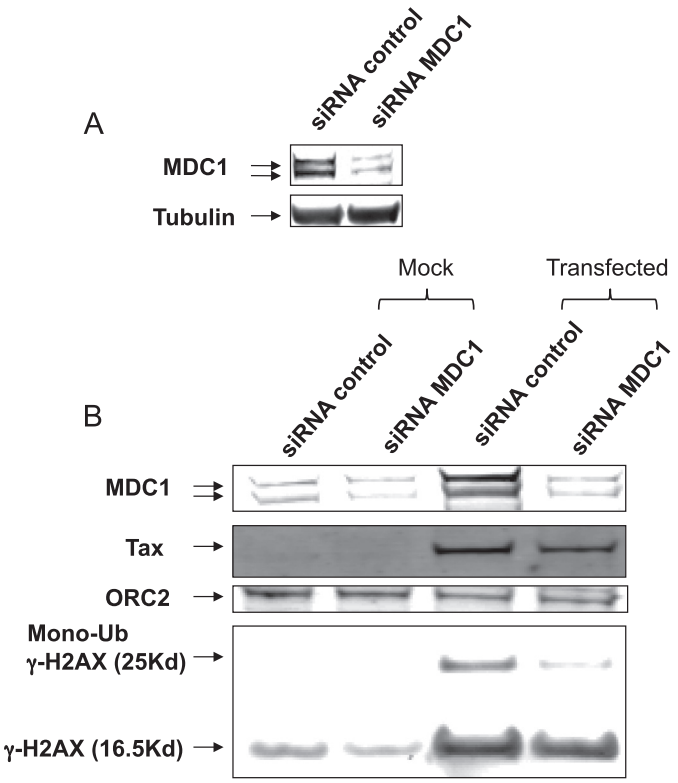

FIGURE 8. **siRNA suppression of MDC1 inhibits Tax-induced DDR signaling.** *A*, efficient suppression of endogenous MDC1 via siRNA. The cells were treated with either control siRNA or siRNA specific for MDC1 (indicated). Whole cell lysates were subjected to SDS-PAGE followed by Western analysis. Shown is expression of MDC1 and tubulin (indicated). *B*, knockdown of MDC1 impairs Tax-mediated DDR signal. The cells were treated with control siRNA or MDC1-specific siRNA and then either mock transfected or transfected to express Tax (indicated). Chromatin fractions were then isolated and subjected to SDS-PAGE separation and analysis by Western blot. Shown is the expression of endogenous MDC1, monoubiquitylated γ-H2AX, and γ-H2AX. Also shown is the expression of Tax protein. The expression of Orc2 was performed for normalization of the chromatin fraction.

gene. Oncogenesis is driven through the activities of a viral protein with oncogenic properties. In fact, the activities ascribed to the HTLV-1 Tax protein are varied and likely reflect the role of this protein in both the biology of the virus and in virus-host interaction (44–47). In regards to a potential oncogenic function, Tax again displays a great variety of activities, although the exact mechanism of action is unknown. One consistent observation has been that expression of Tax correlates with genomic instability in both *in vitro* and *ex vivo* models. Furthermore, Tax-dependent genomic instability is observed in preneoplastic cell isolates and is a precondition to cellular transformation (9, 48). Thus, expression of Tax fulfills the first condition, loss of genomic integrity, of a DNA damage model for cancer (49).

A variety of mechanisms have emerged to explain how oncogenes lead to cancer. In the DNA damage model, an oncogene acts through increased replication to induce DNA damage primarily as double-strand breaks caused by collapse of replicative forks (50, 51). This process would result in genomic instability but would also activate checkpoints via Chk2/Chk1 and subsequently p53-mediated apoptosis/senescence. Overcoming this transformation block is often accomplished through mutation in p53. We present a scenario by which the viral oncogene Tax sequesters DDR factors, thus competing with damage-induced DDR. This competition-based model provides for a mechanistic path to genomic instability through repression of DDR. Interestingly, because we had previously established that Chk2 is also one of the recruited DDR proteins, this model may explain how HTLV-1-infected cells eventually surmount the checkpoint block to cellular transformation.

Suppression of repair by Tax has been proposed as a mechanism for disrupting normal cellular genomic integrity. The consistent observation that Tax-expressing cells display increased mutation frequency in the absence of a direct DNA damage activity drives this repression-of-repair concept. Although a variety of reported Tax activities might indirectly impact the repair process (8), there is support for more direct interplay. Overexpression of Tax can repress base excision and nucleotide excision repair (13, 14) potentially as a result of repression of repair genes (12, 52). Recently, Chandhasin *et al.* (53) clearly demonstrated that repair of double-stranded breaks is impaired in Tax-expressing cells. These authors observed premature cessation of ATM activity and suboptimal recruitment of MDC1 to sites of DNA damage. Our observation that Tax binds to and competitively recruits MDC1 into TSS provides a model that explains these observations. In our model, Tax bridges the formation of a damage-independent DDR foci by recruitment of MDC1. The C-terminal half of Tax binds to MDC1, and the N-terminal half serves as a subcellular localization signal to an as yet undefined chromatin region. Because it has already been established that tethering of MDC1 alone to chromatin can nucleate a DDR and foci formation (38), it is logical that targeting of MDC1 to chromatin by Tax is sufficient for TSS foci formation and generation of a DDR.

Our characterization of the TSS foci revealed that several classic DDR proteins were present. Specifically, we found, in addition to MDC1, the Tax-dependent recruitment of DNA-PK and BRCA1 into these foci. In addition, we have previously reported on the presence of 53BP1 and Chk2 within these same structures (15, 36). Interestingly, Nbs1 was not recruited to the Tax foci. Nbs1 is a component of the MRN complex that is an early damage recognition factor. The association of MRN with damaged DNA ends has been linked to constitutive phosphorylation of MDC1 (26). However, although it is clear from earlier work (38, 54) that stable association with chromatin can initiate DDR in the absence of damage, it is not clear whether MDC1 alone can recruit MRN. For that matter, these damage-independent DDR have yet to be characterized. Thus, the failure to observe recruitment of Nbs1 into TSS foci is reflective of the fact that these foci are not damage-initiated. In fact, our results suggest that the amplification and persistence of MRN are dependent upon the presence of DNA lesions in addition to MDC1.

We show that both IRIF and TSS exist in separable regions and that these sites compete for DDR proteins such as MDC1. When IR is in excess, MDC1 is recruited away from TSS and to IRIF. However, when recruitment to TSS becomes dominant, the result may be premature dissociation of MDC1 from IRIF. In fact, we show that Tax expression and TSS formation result in a dramatic reduction in IR-induced Nbs1-containing foci. Because the quantitation of IRIF via

measurable Nbs1 foci has been shown to characterize the cellular DDR capacity, our results demonstrate that Tax impairs the repair response through a competitive mechanism. Competition with IRIF and control of DDR activities would be expected to: 1) increase fixed damage by bypass of repair, 2) suppress recognition of catastrophic damage and postpone apoptosis, 3) alter the availability of naïve (responsive) DDR factors, thus impairing the ability of the cell to judge extent of damage, and 4) deregulate the DDR activities to benefit the virus via checkpoint control. The formation of TSS is typical of Tax-expressing cells and has been observed in HTLV-1-tranformed cell lines (34, 55). Therefore, we would expect that competition for recruitment of MDC1 occurs in the context of viral infection. However, the functional impact of DDR sequestration at early infection stages needs to be determined.

We present a novel competition model for a viral oncoprotein to supplant cellular control over DDR to ensure survival of the viral host. This competition-based model allows for a mechanism by which Tax overcomes two barriers to oncogenesis. Sequestration of DDR factors results in repression of repair, resulting in increased mutation frequency and genomic instability. This loss in genomic integrity signals the bypass of the first barrier to cancer development. Typically under these circumstances checkpoint activation would engage p53-mediated apoptosis and cell death and presentation of the second barrier. However, competitive sequestration of DDR factors, which include Chk2, would be expected to suppress checkpoint activation and delay apoptosis. The benefits to the virus are selective survival of the host cell, whereas the trade-off is promotion of oncogenesis. Clearly, other virus-host events contribute to long term infection prior to cellular transformation.

Acknowledgments—We thank Ann Campbell and Aurora Esquela-Kersher for critical editing of the manuscript.

REFERENCES

1. Proietti, F. A., Carneiro-Proietti, A. B., Catalan-Soares, B. C., and Murphy, E. L. (2005) *Oncogene* **24,** 6058–6068
2. Tajima, K. (1998) *Jpn. J. Cancer Res.* **89,** inside front cover
3. Pozzatti, R., Vogel, J., and Jay, G. (1990) *Mol. Cell Biol.* **10,** 413–417
4. Tanaka, A., Takahashi, C., Yamaoka, S., Nosaka, T., Maki, M., and Hatanaka, M. (1990) *Proc. Natl. Acad. Sci. U.S.A.* **87,** 1071–1075
5. Akagi, T., and Shimotohno, K. (1993) *J. Virol.* **67,** 1211–1217
6. Grassmann, R., Berchtold, S., Radant, I., Alt, M., Fleckenstein, B., Sodroski, J. G., Haseltine, W. A., and Ramstedt, U. (1992) *J. Virol.* **66,** 4570–4575
7. Jeang, K. T., Giam, C. Z., Majone, F., and Aboud, M. (2004) *J. Biol. Chem.* **279,** 31991–31994
8. Marriott, S. J., and Semmes, O. J. (2005) *Oncogene* **24,** 5986–5995
9. Sibon, D., Gabet, A. S., Zandecki, M., Pinatel, C., Thête, J., Delfau-Larue, M. H., Rabaaoui, S., Gessain, A., Gout, O., Jacobson, S., Mortreux, F., and Wattel, E. (2006) *J. Clin. Invest.* **116,** 974–983
10. Kamada, N., Sakurai, M., Miyamoto, K., Sanada, I., Sadamori, N., Fukuhara, S., Abe, S., Shiraishi, Y., Abe, T., Kaneko, Y., and Shimoyama, M. (1992) *Cancer Res.* **52,** 1481–1493
11. Miyake, H., Suzuki, T., Hirai, H., and Yoshida, M. (1999) *Virology* **253,** 155–161
12. Jeang, K. T., Widen, S. G., Semmes, O. J., 4th, and Wilson, S. H. (1990) *Science* **247,** 1082–1084
13. Kao, S. Y., and Marriott, S. J. (1999) *J. Virol.* **73,** 4299–4304
14. Philpott, S. M., and Buehring, G. C. (1999) *J. Natl. Cancer Inst.* **91,** 933–942
15. Haoudi, A., Daniels, R. C., Wong, E., Kupfer, G., and Semmes, O. J. (2003) *J. Biol. Chem.* **278,** 37736–37744
16. Haoudi, A., and Semmes, O. J. (2003) *Virology* **305,** 229–239
17. Kasai, T., Iwanaga, Y., Iha, H., and Jeang, K. T. (2002) *J. Biol. Chem.* **277,** 5187–5193
18. Park, H. U., Jeong, J. H., Chung, J. H., and Brady, J. N. (2004) *Oncogene* **23,** 4966–4974
19. Jackson, S. P., and Bartek, J. (2009) *Nature* **461,** 1071–1078
20. Lukas, C., Bartek, J., and Lukas, J. (2005) *Chromosoma* **114,** 146–154
21. Misteli, T., and Soutoglou, E. (2009) *Nat. Rev. Mol. Cell Biol.* **10,** 243–254
22. Dimitrova, N., and de Lange, T. (2006) *Genes Dev.* **20,** 3238–3243
23. Eliezer, Y., Argaman, L., Rhie, A., Doherty, A. J., and Goldberg, M. (2009) *J. Biol. Chem.* **284,** 426–435
24. Lou, Z., Minter-Dykhouse, K., Franco, S., Gostissa, M., Rivera, M. A., Celeste, A., Manis, J. P., van Deursen, J., Nussenzweig, A., Paull, T. T., Alt, F. W., and Chen, J. (2006) *Mol. Cell* **21,** 187–200
25. Minter-Dykhouse, K., Ward, I., Huen, M. S., Chen, J., and Lou, Z. (2008) *J. Cell Biol.* **181,** 727–735
26. Spycher, C., Miller, E. S., Townsend, K., Pavic, L., Morrice, N. A., Janscak, P., Stewart, G. S., and Stucki, M. (2008) *J. Cell Biol.* **181,** 227–240
27. Stucki, M., and Jackson, S. P. (2006) *DNA Repair* **5,** 534–543
28. Xie, A., Hartlerode, A., Stucki, M., Odate, S., Puget, N., Kwok, A., Nagaraju, G., Yan, C., Alt, F. W., Chen, J., Jackson, S. P., and Scully, R. (2007) *Mol. Cell* **28,** 1045–1057
29. Huen, M. S., Grant, R., Manke, I., Minn, K., Yu, X., Yaffe, M. B., and Chen, J. (2007) *Cell* **131,** 901–914
30. Kolas, N. K., Chapman, J. R., Nakada, S., Ylanko, J., Chahwan, R., Sweeney, F. D., Panier, S., Mendez, M., Wildenhain, J., Thomson, T. M., Pelletier, L., Jackson, S. P., and Durocher, D. (2007) *Science* **318,** 1637–1640
31. Marteijn, J. A., Bekker-Jensen, S., Mailand, N., Lans, H., Schwertman, P., Gourdin, A. M., Dantuma, N. P., Lukas, J., and Vermeulen, W. (2009) *J. Cell Biol.* **186,** 835–847
32. Yan, J., and Jetten, A. M. (2008) *Cancer Lett* **271,** 179–190
33. Durkin, S. S., Ward, M. D., Fryrear, K. A., and Semmes, O. J. (2006) *J. Biol. Chem.* **281,** 31705–31712
34. Semmes, O. J., and Jeang, K. T. (1996) *J. Virol.* **70,** 6347–6357
35. Durkin, S. S., Guo, X., Fryrear, K. A., Mihaylova, V. T., Gupta, S. K., Belgnaoui, S. M., Haoudi, A., Kupfer, G. M., and Semmes, O. J. (2008) *J. Biol. Chem.* **283,** 36311–36320
36. Gupta, S. K., Guo, X., Durkin, S. S., Fryrear, K. F., Ward, M. D., and Semmes, O. J. (2007) *J. Biol. Chem.* **282,** 29431–29440
37. Raderschall, E., Golub, E. I., and Haaf, T. (1999) *Proc. Natl. Acad. Sci. U.S.A.* **96,** 1921–1926
38. Soutoglou, E., and Misteli, T. (2008) *Science* **320,** 1507–1510
39. Stucki, M., Clapperton, J. A., Mohammad, D., Yaffe, M. B., Smerdon, S. J., and Jackson, S. P. (2005) *Cell* **123,** 1213–1226
40. Lou, Z., Minter-Dykhouse, K., Wu, X., and Chen, J. (2003) *Nature* **421,** 957–961
41. Fryrear, K. A., Durkin, S. S., Gupta, S. K., Tiedebohl, J. B., and Semmes, O. J. (2009) *J. Virol.* **83,** 5339–5352
42. Mailand, N., Bekker-Jensen, S., Faustrup, H., Melander, F., Bartek, J., Lukas, C., and Lukas, J. (2007) *Cell* **131,** 887–900
43. Shao, G., Lilli, D. R., Patterson-Fortin, J., Coleman, K. A., Morrissey, D. E., and Greenberg, R. A. (2009) *Proc. Natl. Acad. Sci. U.S.A.* **106,** 3166–3171
44. Grassmann, R., Aboud, M., and Jeang, K. T. (2005) *Oncogene* **24,** 5976–5985
45. Nyborg, J. K., Egan, D., and Sharma, N. (2010) *Biochim. Biophys. Acta* **1799,** 266–274
46. Peloponese, J. M., Jr., Kinjo, T., and Jeang, K. T. (2007) *Int. J. Hematol.* **86,** 101–106
47. Saggioro, D., Silic-Benussi, M., Biasiotto, R., D'Agostino, D. M., and Ciminale, V. (2009) *Front. Biosci.* **14,** 3338–3351
48. Zane, L., Sibon, D., Mortreux, F., and Wattel, E. (2009) *Front. Biosci.* **14,** 3935–3941
49. Halazonetis, T. D., Gorgoulis, V. G., and Bartek, J. (2008) *Science* **319,**

1352–1355
50. Bartkova, J., Rezaei, N., Liontos, M., Karakaidos, P., Kletsas, D., Issaeva, N., Vassiliou, L. V., Kolettas, E., Niforou, K., Zoumpourlis, V. C., Takaoka, M., Nakagawa, H., Tort, F., Fugger, K., Johansson, F., Sehested, M., Andersen, C. L., Dyrskjot, L., Ørntoft, T., Lukas, J., Kittas, C., Helleday, T., Halazonetis, T. D., Bartek, J., and Gorgoulis, V. G. (2006) *Nature* **444,** 633–637
51. Di Micco, R., Fumagalli, M., Cicalese, A., Piccinin, S., Gasparini, P., Luise, C., Schurra, C., Garre, M., Nuciforo, P. G., Bensimon, A., Maestro, R., Pelicci, P. G., and d'Adda di Fagagna, F. (2006) *Nature* **444,** 638–642
52. Edwards, D. C., and Marriott, S. J. (2008) *J. Virol.* **82,** 11714–11722
53. Chandhasin, C., Ducu, R. I., Berkovich, E., Kastan, M. B., and Marriott, S. J. (2008) *J. Virol.* **82,** 6952–6961
54. Bonilla, C. Y., Melo, J. A., and Toczyski, D. P. (2008) *Mol. Cell* **30,** 267–276
55. Park, H. U., Jeong, S. J., Jeong, J. H., Chung, J. H., and Brady, J. N. (2006) *Oncogene* **25,** 438–447